THE JOURNAL OF PHYSICAL CHEMISTRY Letters

Letter

pubs.acs.org/JPCL

Frustrated Solvation Structures Can Enhance Electron Transfer Rates

Richard C. Remsing,*[,†,§] Ian G. McKendry,[‡,§] Daniel R. Strongin,[‡,§] Michael L. Klein,[†,§] and Michael J. Zdilla[‡,§]

[†]Institute for Computational Molecular Science, [‡]Department of Chemistry, and [§]Center for the Computational Design of Functional Layered Materials, Temple University, Philadelphia, Pennsylvania 19122, United States

Supporting Information

ABSTRACT: Polar surfaces can interact strongly with nearby water molecules, leading to the formation of highly ordered interfacial hydration structures. This ordering can lead to frustration in the hydrogen bond network, and, in the presence of solutes, frustrated hydration structures. We study frustration in the hydration of cations when confined between sheets of the water oxidation catalyst manganese dioxide. Frustrated hydration structures are shown to have profound effects on ion-surface electron transfer through the enhancement of energy gap fluctuations beyond those expected from Marcus theory. These fluctuations are accompanied by a concomitant increase in the electron transfer rate in Marcus's normal regime. We demonstrate the generality of this phenomenon—enhancement of energy gap fluctuations due to frustration—by introducing a charge frustrated XY model, likening the hydration structure of confined cations to topological defects. Our findings shed light on recent experiments suggesting that water oxidation rates depend on the cation charge and Mn-oxidation state in these layered transition metal oxide materials.

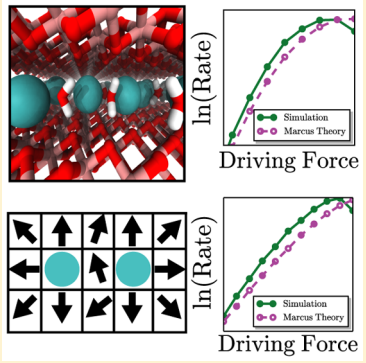

Competition among interactions can lead to highly degenerate ground states in physical systems that are unable to minimize all components of their energy simultaneously. This phenomena—*frustration*—is quite ubiquitous and underpins many physical processes, including glass formation,[1,2] proton disorder in ice,[3] self-assembly,[4] and various aspects of magnetism.[1,3,5] In this work, we detail a realization of frustrated interactions existing in aqueous solutions confined between sheets of manganese dioxide (MnO_2).

Materials made of stacked two-dimensional sheets of MnO_2 with a single layer of water and cations confined between them, known as birnessites, are promising catalysts for the oxidation of water.[6−12] These layered materials present a unique, confined interlayer environment that is conducive to redox chemistry. Indeed, birnessites also facilitate redox reactions involving a variety of ionic species.[13] However, little is known regarding the microscopic structure between the sheets, and even less about the influence of confinement on reactivity.

We show that an interplay between surface water, water−ion, and ion−ion interactions leads to frustrated hydration structures. This frustration enhances the rate of electron transfer between dissolved solutes and MnO_2. We further illustrate that this rate enhancement is a general consequence of frustrated solvation structures through the development and numerical study of a charge frustrated XY model that minimally embodies the underlying physics of the confined aqueous solution. Thus, the analysis presented in this study is expected to have relevance to other redox active layered materials.

We have carried out classical mechanical molecular dynamics (MD) simulations of birnessite with water and K^+ confined between the layers with GROMACS5[14] and the CLAYFF force field[15] to describe the transition metal oxide surface, suitably modified for Mn.[16] MnO_2 was fixed in its crystal structure[17] with the distance between sheets set to its equilibrium value for this model.[16] Note that we do not consider the possibility and role of cation vacancies, which can often appear in birnessite. An open system was mimicked by leaving the edges of the birnessite open to water reservoirs, allowing exchange between the interlayer regions, illustrated in Figure 1A. All simulations were conducted in the canonical ensemble at T = 300 K using the canonical velocity-rescaling thermostat,[18] and a constant coexistence pressure was maintained by including water−vapor interfaces on either side of the reservoirs. Water was modeled using the extended simple point charge (SPC/E) model,[19] in accordance with CLAYFF. The ions were described using the Smith and Dang parameters[20] for K^+; we expect the existence of frustration to be independent of ion type, although the amount of frustration will quantitatively depend on the nature of the ions.

Negatively charged MnO_2 sheets interact strongly with water, competing with its hydrogen-bond network. Such competition can lead to frustration in liquid ordering near surfaces.[21] Water confined to the birnessite interlayer is indeed highly ordered, in a manner that is incommensurate with the formation of water−water H-bonds, as highlighted in Figure 1. The substantial ordering of water molecules in the interlayer is supported by experimentally determined IR spectra presented in the Supporting Information (SI), in which sharpened peaks relative

Received: October 12, 2015
Accepted: November 16, 2015
Published: November 16, 2015

DOI: 10.1021/acs.jpclett.5b02277
J. Phys. Chem. Lett. 2015, 6, 4804−4808

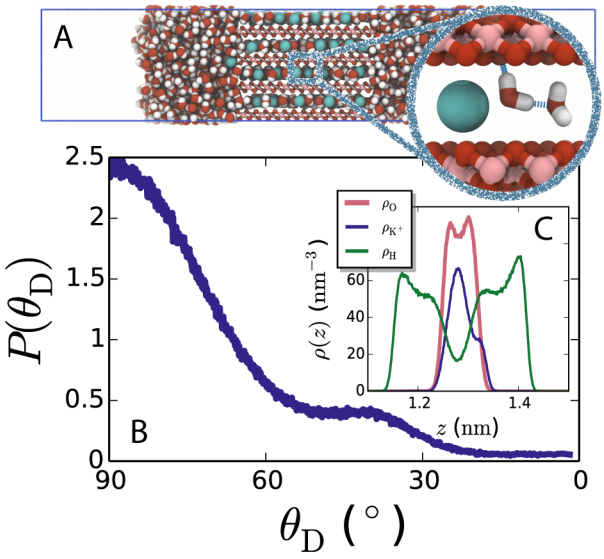

Figure 1. (A) The simulation cell (blue lines) includes four layers of MnO_2 oriented perpendicular to the z-axis and reservoirs of water in each x-direction to allow for exchange of solution between layers. Water-vapor interfaces maintain the system at coexistence pressure. Oxygen is colored red, hydrogen is white, Mn is pink, and K^+ is green. (B) The probability distribution of the angle made by the water dipole moment and the z-axis, θ_D, suggests two dominant populations of water, depicted in the inset, which shows a snapshot of the two major configurations of water molecules in the interlayer region. The leftmost water is the minor configuration, while the rightmost water exemplifies the dominant population. (C) The density $\rho(z)$ in a single interlayer indicates that water O atoms and K^+ occupy the same plane, while H atoms are positioned above and below this plane.

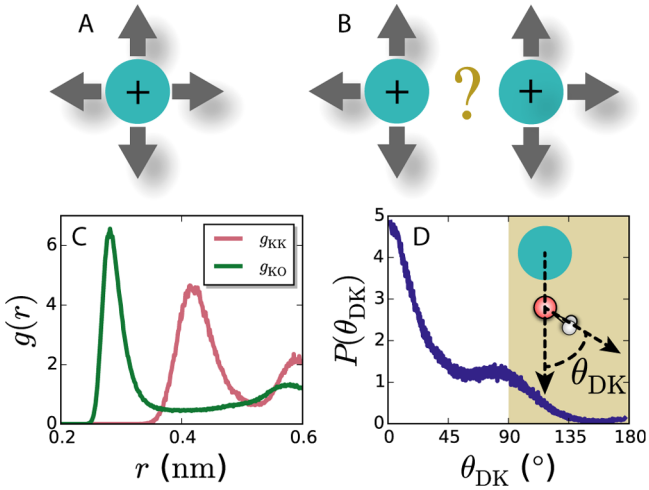

Figure 2. (A) Sketch of the ideal cation hydration structure in a two-dimensional dipolar fluid, where the green circle corresponds to a cation, and black arrows correspond to dipoles pointing away from the ion. (B) Frustration arises when cations share a hydration shell, as is the case in the interlayer. A water molecule between two cations cannot adopt a configuration corresponding to a unique lowest energy ground state, indicated by the yellow question mark. (C) In-plane pair correlation functions $g(r)$ of K^+ and O atoms around a cation suggest shared hydration shells. (D) Probability distributions of the angle made by water dipoles and the vector connecting the cation and water indicate the existence of charge−dipole repulsion in cation hydration shells.

to those in bulk water suggest highly ordered water structures. We find that a single interlayer plane is occupied by both water oxygen sites and cations, consistent with crystallographic structural descriptions of birnessite[17] and evidenced by overlapping peaks in the number densities of water oxygen sites and K^+ shown in Figure 1C, $\rho_O(z)$ and $\rho_K(z)$, respectively.

The density of hydrogen sites, $\rho_H(z)$, displays peaks on either side of the oxygen density peak, suggesting strong orientational ordering that points hydrogen atoms toward the surface. Analysis of the probability distribution of the angle formed by the dipole moment vector of water and the surface normal, $P(\theta_D)$, shown in Figure 1B, indicates that an interlayer water predominantly adopts an orientation wherein its dipole lies in the plane parallel to the confining surfaces. A less probable orientation is also observed, in which waters point a single O−H bond parallel to the surface in an effort to form water−water H-bonds, as illustrated by the central water of the snapshot in Figure 1. The predominant orientation is unable to form H-bonds with neighboring waters in the same orientation, illustrated by the rightmost water in Figure 1. The extensively ordered water confined within the interlayer of birnessite can thus be effectively considered a two-dimensional fluid of dipoles by focusing on this dominant orientation.

The strong two-dimensional ordering of water molecules has profound consequences on ion hydration within the interlayer region. At infinite dilution, a two-dimensional fluid of dipoles would preferentially solvate a cation in a configuration reminiscent of that shown in Figure 2A; dipoles would surround the cation, all pointing directly away from the positively charged solute. The solution confined between MnO_2 layers, however, is not close to infinite dilution, with roughly one cation for every three water molecules. Hence, cations often share hydration shells, as evidenced by the pair distribution functions, $g(r)$, shown in Figure 2C, in which the first peak in the ion−ion $g(r)$ occurs near the first minimum of the water−ion correlation function.

Frustration arises when two cations share a hydration shell in this two-dimensional fluid, as schematically illustrated in Figure 2B, where the central, shared dipole (water) cannot adopt a configuration that leaves it in a unique ground state. Water instead adopts a range of orientations around cations, as evidenced by the probability distribution of the angle made by the dipole vector and the water−ion distance vector, $P(\theta_{DK})$, shown in Figure 2D. The first peak at $\theta_{DK} \approx 0°$ corresponds to the ideal hydration structure. The secondary peak just below $\theta_{DK} = 90°$ arises mainly from frustration, with a component due to the small population of waters that participate in water−water H-bonds. Importantly, $P(\theta_{DK})$ is nonzero for $\theta_{DK} > 90°$, indicating the presence of significant dipole-charge repulsions, as one would expect in such a frustrated system.

Frustrated interactions can lead to enhanced fluctuations with respect to unfrustrated systems; here fluctuations in water orientation and cation coordination numbers are strongly affected by frustration. Such fluctuations play a critical role in solvent-mediated processes, like the electron transfer (ET) reactions involved in water oxidation.[22−24] We consider the general ET process

$$M^q + Mn^{q_{Mn}} \rightarrow M^{q+1} + Mn^{q_{Mn}-1} \quad (1)$$

effectively modeling transfer of an electron from a cation to the nearest Mn site of the surface, where q_{Mn} is the charge on Mn; qualitatively similar effects are found for reduction of M. Here, M represents a general redox active (metal) ion, conceptually different from K^+, in the sense that it can readily undergo ET,

DOI: 10.1021/acs.jpclett.5b02277
J. Phys. Chem. Lett. 2015, 6, 4804−4808

but it is modeled with K^+ parameters ($q = +1$) to avoid other sources of complexity. Thus, we treat all cations the same and expect qualitatively similar results from other point charge models. In reality, more complex species like Ce^{4+} can be involved in redox processes,[12] which may require more detailed models.

We characterize the ET process using the energy gap ΔE as an order parameter, where

$$\Delta E(\bar{\mathbf{R}}) = \mathcal{H}_1(\bar{\mathbf{R}}) - \mathcal{H}_0(\bar{\mathbf{R}}) \tag{2}$$

defines the energy gap in configuration $\bar{\mathbf{R}}$ as the difference between the Hamiltonians, $\mathcal{H}_\lambda$, of the oxidized (M^{+2}, $\lambda = 1$) and reduced (M^+, $\lambda = 0$) states, and λ is a coupling parameter that linearly transforms the system between states. The energy gap provides an accurate reduced description of ET processes.[22−24] Distributions of ΔE were computed using umbrella sampling[25] with the coupled cation and Mn charges as the biasing parameter to adequately sample λ-space, and $P(\Delta E)$ was obtained using UWHAM.[26]

Distributions of the energy gap obtained in both the oxidized and reduced states are compared to the Gaussian distributions predicted by the celebrated Marcus theory[24] of ET in Figure 3A. Fluctuations in ΔE are significantly enhanced by frustrated

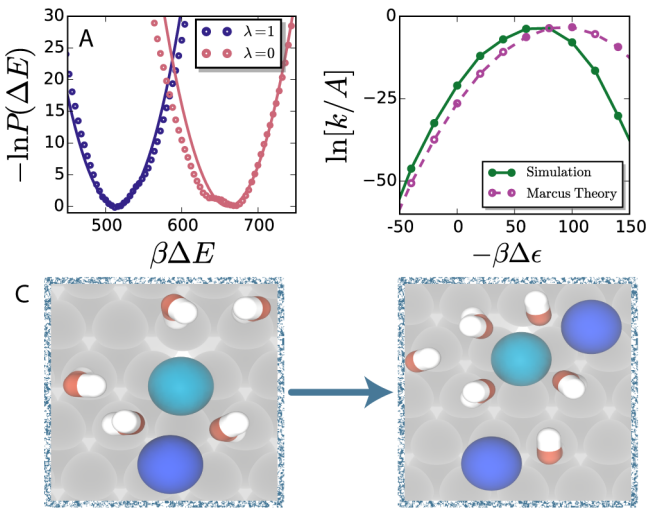

Figure 3. (A) Distributions of the energy gap, ΔE, obtained from simulations (points) are distinctly non-Gaussian, even near the mean, while Marcus theory predicts Gaussian statistics (lines). (B) Enhanced energy gap fluctuations lead to faster rate constants in the normal regime (left of the peak), but a pronounced reduction in the inverted regime (right of the peak), with respect to Marcus theory predictions. (C) A change in the charge of the redox ion M (green) breaks the symmetry between it and the remaining cations (dark blue), such that frustration no longer exists in its hydration shell, and waters become oriented in an ideal fashion (see Figure 2A).

hydration, leading to non-Gaussian statistics of ΔE, even near the mean for the $\lambda = 0$ distribution. Deviations from Marcus theory are smaller in the oxidized ($\lambda = 1$) state because frustration no longer exists around the oxidized divalent ion. Oxidation breaks the symmetry among cations in the confined space, and water molecules in the hydration shell of the redox ion are no longer frustrated. These waters adopt an ideal, minimum energy-like configuration, as highlighted by the snapshots in Figure 3C. This symmetry breaking is accompanied by large changes in the coordination of both water and cations around the redox species, with the coordination number of water molecules increasing from 1.6 to 2.8 upon oxidization and the position of the cation coordination shell shifting to larger distances by nearly 0.5 Å due to increasing repulsions from the ordered hydration shell. In the absence of frustration, similar changes in coordination number between end states,[23] or structural changes brought about by interfaces,[27] lead to significantly smaller deviations from Marcus theory. We also note that enhancements of energy gap fluctuations similar to those observed here have been achieved through alternative mechanisms, for example, by having ET occur in a ferroelectric liquid with a net macroscopic polarization.[28]

Enhanced fluctuations in ΔE lead to significant differences in the height of the free energy barrier for ET with respect to Marcus theory predictions, resulting in dramatic changes to reaction rates. We estimate the reaction rate constant k according to $k(\Delta\epsilon) = A\exp(-\beta\Delta G^{\ddagger})$, where $\Delta G^{\ddagger}$ is the height of the free energy barrier, and A is a constant related to the probability of electron tunneling,[24] and its determination is beyond the scope of the current work; we focus here on the barrier height. The thermodynamic driving force for ET, $\Delta\epsilon$, is equivalent to the vertical displacement between the minima of $-\ln P(\Delta E)$ for $\lambda = 0$ and $\lambda = 1$, and we estimate k/A for a range of $\Delta\epsilon$ by displacing these distributions vertically with respect to one another. In Marcus's normal regime, to the left of the maximum in $\ln k/A$, ET rates are significantly increased by the enhanced fluctuations arising from frustration, as shown in Figure 3B. In contrast, rates are severely decreased in the inverted regime (right of the maximum), which is particularly noteworthy because Marcus theory often underestimates rates in this regime.[24]

The effects of frustration on energy gap fluctuations is a general phenomena. This is illustrated by recalling the picture of confined water as a two-dimensional fluid of dipoles, where a single water is uniquely described by its position, $\mathbf{r}$, and dipolar orientation, θ, while ions are described simply by their position. Water in this confined space is reminiscent of a two-dimensional XY model.[29] In this analogy, ion hydration induces the formation of topological defects, with the hydration of a single cation inducing the formation of a vortex with a winding number of one (Figure 2A). However, unlike the situation in a uniform XY model, vortices cannot annihilate, and the number of ions in the system fixes the concentration of defects. These defects have explicit repulsions between one another, in addition to those mediated by the solvent.

A minimal description of the physics underlying the behavior of the birnessite interlayer region can thus be embodied by a *charge frustrated XY model* with the Hamiltonian $\mathcal{H} = \mathcal{H}_{XY} + \mathcal{H}_q + \mathcal{H}_I$, where

$$\mathcal{H}_{XY} = -J_{XY}\sum_{\langle i,j\rangle}\cos(\theta_i - \theta_j)\Theta(1 - t_i)\Theta(1 - t_j) \tag{3}$$

is the Hamiltonian for the solvent−solvent (XY) interactions. Here, J_{XY} sets the energy scale, the sum is restricted to nearest-neighbors, $t_i = 0$ if the site corresponds to solvent, $t_i = 1$ for an ion, and $\Theta(x)$ is the Heaviside function. The interactions between ionic sites are described by the charge-portion of the Hamiltonian,[4]

$$\mathcal{H}_q = \frac{q^2}{2}\sum_{i\neq j} v(r_{ij})s_i s_j t_i t_j \tag{4}$$

DOI: 10.1021/acs.jpclett.5b02277
J. Phys. Chem. Lett. 2015, 6, 4804−4808

where $s_i = +1$ (-1) if site i represents a cation (anion), $v(r_{ij})$ is the two-dimensional Coulomb potential that depends on the scalar distance r_{ij} between sites i and j, and q is an effective charge on the site related to the Debye screening length in the solution.[4] The interactions between the XY and charged sites are described by

$$\mathcal{H}_I = -J_I \sum_{\langle i,j \rangle} s_i t_i (1 - t_j) \cos \phi_{ij} \quad (5)$$

where ϕ_{ij} is the angle made by the vector connecting sites i and j and the unit vector of the XY site, such that $\cos \phi_{ij} = 1$ when spin j points directly away from site i. This interaction favors the formation of a vortex with a winding number of one with an ion at its core.

Frustration in this model arises from a competition between solute−solvent and solvent−solvent interactions: $\mathcal{H}_I$ favors the formation of vortices, while $\mathcal{H}_{XY}$ tends to align spins, disfavoring defect formation. Electrostatic repulsions, $\mathcal{H}_q$, maintain a nearly constant number of defects in the system by inhibiting the clustering of cationic sites.

We perform Metropolis Monte Carlo simulations of the charge frustrated XY model on a 10×10 square lattice at $k_B T/J_{XY} = 0.5$ and monitor the energy gap in complete analogy with the above-described atomistic simulation, where λ couples to s_i of the redox site. Both single particle spin flip (for XY sites) and two particle swap moves were employed. We set $J_I = J_{XY}$ for simplicity. ET in the lattice is studied by changing s_i of a single, fixed site from 1 to 2500, resulting in a change of spin $\Delta s = 2499$, chosen to yield a change in coordination structure qualitatively similar to that in the atomistic system.

Distributions of ΔE obtained from the charge frustrated XY model, shown in Figure 4A, exhibit enhanced fluctuations in the direction of charging with respect to those expected from Marcus theory, qualitatively similar to the atomistic results. These enhanced fluctuations arise from frustrated solvation environments. Moreover, the enhanced fluctuations lead to rate constants in qualitative agreement with the atomistic results; rates in the normal (inverted) regime are increased (decreased) with respect to Marcus theory, as illustrated in Figure 4B. This model will allow for efficient sampling of parameter space to suggest strategies for using energy gap fluctuations to control ET rates, which is left for future study.

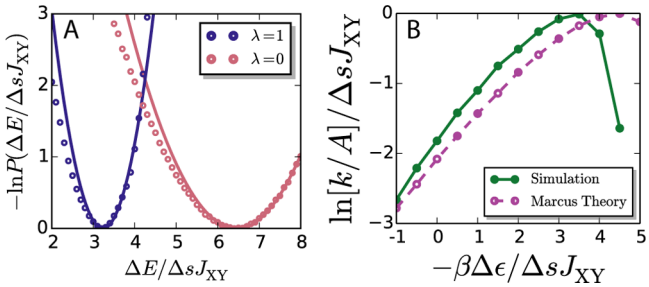

Figure 4. (A) Fluctuations in the energy gap of the charge frustrated XY model are enhanced in the direction of charging, consistent with what is observed for electron transfer in the interlayer of MnO_2. Lines are Gaussian fits to the high ΔE side of the data. (B) The rate constant is increased in the normal regime and decreased in the inverted regime with respect to Marcus theory predictions, taken from the Gaussian fits. Energies are scaled by the product of the XY model energy scale, J_{XY}, and the change in the spin of the redox site, Δs.

The reduced description provided by the charge frustrated XY model relies on the ordering of water into an effective two-dimensional dipolar fluid. In the atomistic system, however, a small population of confined molecules do not orient their dipole parallel to the surface and instead point an O−H bond in this direction. This latter population of water molecules can be reduced by tuning water−ion and water−surface interactions, leading to more frustration in the system.

This perspective helps explain recent experimental findings regarding reactivity in layered MnO_2 systems. Experiments have suggested that the presence of multivalent ions leads to enhanced reactions rates for the reduction of redox ions and the oxidation of water beyond that obtained with monovalent cations.[10,13] Increasing cation−water interactions within the confined interlayer region tends to enhance the ordering of water molecules, which align their dipoles parallel to the surface more than observed in the monovalent case. Additionally, decreasing the interlayer spacing with smaller ions will increase the ordering of confined water molecules. The increase in orientational order should create more frustration, which is accompanied by a concomitant enhancement of fluctuations in ΔE and the ET rate in the normal regime.

Similar increases in reactivity have been observed when decreasing the average oxidation state of MnO_2.[12] In the context of the simple, empirical models used here, a reduction in the oxidation state of the surface simply increases the magnitude of the negative charge distributed over the surfaces that are confining water. This increase in charge should lead to stronger surface water interactions, and thus an increase in frustration and ET rates. Indeed, the experimental and simulated IR spectra displayed in the SI show a sharpening of peaks upon lowering the average oxidation state of birnessite, consistent with increased ordering of the confined water molecules. The nature of the cations in solution and the Mn oxidation state undoubtedly have additional profound chemical effects, not limited to altering the structure of the material through Jahn−Teller effects, but our findings indicate that solvation effects should play a significant role in controlling reaction rates in these materials.

■ ASSOCIATED CONTENT

Supporting Information

The Supporting Information is available free of charge on the ACS Publications website at DOI: 10.1021/acs.jpclett.5b02277.

Experimental and simulated IR spectra for different amounts of water ordering in birnessite and the details regarding their determination. (PDF)

■ AUTHOR INFORMATION

Corresponding Author

*E-mail: rremsing@temple.edu.

Notes

The authors declare no competing financial interest.

■ ACKNOWLEDGMENTS

This work was supported primarily as part of the Center for the Computational Design of Functional Layered Materials, an Energy Frontier Research Center funded by the U.S. Department of Energy, Office of Science, Basic Energy Sciences under Award #DE-SC0012575. A portion of the computations were performed on resources provided by the National Science Foundation through major research instrumentation grant

DOI: 10.1021/acs.jpclett.5b02277
J. Phys. Chem. Lett. 2015, 6, 4804−4808

number CNS-09-58854. We thank Jianwei Sun and Suri Vaikuntanathan for insightful discussions.

REFERENCES

(1) Binder, K.; Young, A. P. Spin glasses: Experimental Facts, Theoretical Concepts, and Open Questions. *Rev. Mod. Phys.* **1986**, *58*, 801−976.
(2) Tarjus, G.; Kivelson, S. A.; Nussinov, Z.; Viot, P. The Frustration-Based Approach of Supercooled Liquids and the Glass Transition: a Review and Critical Assessment. *J. Phys.: Condens. Matter* **2005**, *17*, R1143−R1182.
(3) Henley, C. L. The "Coulomb phase" in Frustrated Systems. *Annu. Rev. Condens. Matter Phys.* **2010**, *1*, 179−210.
(4) Wu, D.; Chandler, D.; Smit, B. Electrostatic Analogy for Surfactant Assemblies. *J. Phys. Chem.* **1992**, *96*, 4077−4083.
(5) De'Bell, K.; MacIsaac, A. B.; Whitehead, J. P. Dipolar Effects in Magnetic Thin Films and Quasi-Two-Dimensional Systems. *Rev. Mod. Phys.* **2000**, *72*, 225−257.
(6) Lopano, C. L.; Heaney, P. J.; Post, J. E.; Hanson, J.; Komarneni, S. Time-Resolved Structural Analysis of K- and Ba-Exchange Reactions with Synthetic Na-Birnessite using Synchrotron X-ray Diffraction. *Am. Mineral.* **2007**, *92*, 380−387.
(7) Takashima, T.; Hashimoto, K.; Nakamura, R. Inhibition of Charge Disproportionation of MnO_2 Electrocatalysts for Efficient Water Oxidation under Neutral Conditions. *J. Am. Chem. Soc.* **2012**, *134*, 18153−18156.
(8) Wiechen, M.; Zaharieva, I.; Dau, H.; Kurz, P. Layered Manganese Oxides for Water-Oxidation: Alkaline Earth Cations Influence Catalytic Activity in a Photosystem II-like Fashion. *Chem. Sci.* **2012**, *3*, 2330−2339.
(9) Robinson, D. M.; Go, Y. B.; Mui, M.; Gardner, G.; Zhang, Z.; Mastrogiovanni, D.; Garfunkel, E.; Li, J.; Greenblatt, M.; Dismukes, G. C. Photchemical Water Oxidation by Crystalline Polymorphs of Manganese Oxides: Structural Requirements for Catalysts. *J. Am. Chem. Soc.* **2013**, *135*, 3494−3501.
(10) Frey, C. E.; Wiechen, M.; Kurz, P. Water-Oxidation Catalysis by Synthetic Manganese Oxides-Systematic Variations of the Calcium Birnessite Theme. *Dalton Trans.* **2014**, *43*, 4370−4379.
(11) Wiechen, M.; Najafpour, M. M.; Allakhverdiev, S. I.; Spiccia, L. Water Oxidation Catalysis by Manganese Oxides: Learning from Evolution. *Energy Environ. Sci.* **2014**, *7*, 2203−2212.
(12) McKendry, I. G.; Kondaveeti, S. K.; Shumlas, S. L.; Strongin, D. R.; Zdilla, M. J. Decoration of the Layered Manganese Oxide Birnessite with Mn(II/III) Gives a New Water Oxidation Catalyst with Fifty-Fold Turnover Number Enhancement. *Dalton Trans.* **2015**, *44*, 12981−12984.
(13) Banerjee, D.; Nesbitt, H. W. Oxidation of aqueous Cr(III) at birnessite surfaces: Constraints on reaction mechanism. *Geochim. Cosmochim. Acta* **1999**, *63*, 1671−1687.
(14) Hess, B.; Kutzner, C.; van der Spoel, D.; Lindahl, E. GROMACS 4: Algorithms for Highly Efficient, Load-Balanced, and Scalable Molecular Simulation. *J. Chem. Theory Comput.* **2008**, *4*, 435−447.
(15) Cygan, R. T.; Liang, J.-J.; Kalinichev, A. G. Molecular Models of Hydroxide, Oxyhydroxide, and Clay Phases and the Development of a General Force Field. *J. Phys. Chem. B* **2004**, *108*, 1255−1266.
(16) Cygan, R. T.; Post, J. E.; Heaney, P. J.; Kubicki, J. D. Molecular Models of Birnessite and Related Hydrated Layered Minerals. *Am. Mineral.* **2012**, *97*, 1505−1514.
(17) Post, J. E.; Veblen, D. R. Crystal Structure Determinations of Synthetic Sodium, Magnesium, and Potassium Birnessite using TEM and the Rietveld Method. *Am. Mineral.* **1990**, *75*, 477−489.
(18) Bussi, G.; Donadio, D.; Parrinello, M. Canonical Sampling Through Velocity Rescaling. *J. Chem. Phys.* **2007**, *126*, 014101.
(19) Berendsen, H. J. C.; Grigera, J. R.; Straatsma, T. P. The Missing Term in Effective Pair Potentials. *J. Phys. Chem.* **1987**, *91*, 6269−6271.
(20) Smith, D. E.; Dang, L. X. Computer Simulations of NaCl Association in Polarizable Water. *J. Chem. Phys.* **1994**, *100*, 3757−3766.
(21) Limmer, D. T.; Willard, A. P.; Madden, P.; Chandler, D. Hydration of Metal Surfaces can be Dynamically Heterogeneous and Hydrophobic. *Proc. Natl. Acad. Sci. U. S. A.* **2013**, *110*, 4200−4205.
(22) Ayala, R.; Sprik, M. A Classical Point Charge Model Study of System Size Dependence of Oxidation and Reorganization Free Energies in Aqueous Solution. *J. Phys. Chem. B* **2008**, *112*, 257−269.
(23) Blumberger, J.; Tavernelli, I.; Klein, M. L.; Sprik, M. Diabatic Free Energy Curves and Coordination Fluctuations for the Aqueous Ag^+Ag^{2+} Redox Couple: a Biased Born-Oppenheimer Molecular Dynamics Investigation. *J. Chem. Phys.* **2006**, *124*, 064507.
(24) Marcus, R. A. Electron Transfer Reactions in Chemistry. Theory and Experiment. *Rev. Mod. Phys.* **1993**, *65*, 599−610.
(25) Torrie, G. M.; Valleau, J. P. Nonphysical Sampling Distributions in Monte Carlo Free-Energy Estimation: Umbrella Sampling. *J. Comput. Phys.* **1977**, *23*, 187−199.
(26) Tan, Z.; Gallicchio, E.; Lapelosa, M.; Levy, R. M. Theory of Binless Multi-State Free Energy Estimation with Applications to Protein-Ligand Binding. *J. Chem. Phys.* **2012**, *136*, 144102.
(27) Rose, D. A.; Benjamin, I. Molecular Dynamics of Adiabatic and Nonadiabatic Electron Transfer at the Metal-Water Interface. *J. Chem. Phys.* **1994**, *100*, 3545−3555.
(28) Matyushov, D. V. Reorganization Asymmetry of Electron Transfer in Ferroelectric Media and Principles of Artifical Photosynthesis. *J. Phys. Chem. B* **2006**, *110*, 10095−10104.
(29) Chaikin, P. M.; Lubensky, T. C. *Principles of Condensed Matter Physics*; Cambridge University Press: Cambridge, U.K., 1995.

DOI: 10.1021/acs.jpclett.5b02277
J. Phys. Chem. Lett. 2015, 6, 4804−4808